Sports Engineering (2024) 27:27
https://doi.org/10.1007/s12283-024-00471-7

ORIGINAL ARTICLE

Accounting for friction in the mechanical testing of athletics tracks

Luca Andena[1,2] · Riccardo Gobbi[1,2] · Paolo Meda[1,2] · Samuele Zalaffi[1] · Andrea Marenghi[3]

Accepted: 26 July 2024

Abstract
This investigation deals with the problem of identifying the mechanical behaviour of rubbers from compression tests, performed on specimens having unfavorable geometry. A typical situation is that of flat specimens obtained from high-friction sports surfaces. To this purpose, experimental tests were conducted, aimed at measuring friction under various conditions and evaluating its effect on the compressive behavior of different rubber samples. The experimental results have been interpreted in view of an existing analytical model proposed by Gent and coworkers. The method was shown to be valid within a relatively broad range of conditions (in terms of materials, lubrication and aspect ratio). Its application allowed the creation of virtual "frictionless" curves, by rescaling experimental data for the stiffening factor predicted by Gent model. These curves represent more closely the intrinsic material behaviour, removing the large frictional contribution present in the experimental tests, and can be used as a more reliable input for numerical simulations.

Keywords Friction · Mechanical testing · Rubber · Compression · Sports surfaces

1 Introduction and aim of the work

Synthetic sports surfaces represent the de facto standard for high-level athletics competitions worldwide. These polymeric systems offer several advantages over unbound mineral surfaces and natural grass, providing an optimal combination of superior dynamic characteristics and minimal maintenance. Two main families of synthetic surfaces are allowed by existing regulations, set by World Athletics: prefabricated sheets and in-situ systems [1]. While many surfacing products belonging to both categories are available, prefabricated surfaces are frequently selected in major international athletics events, including all the Olympic Games held since Montreal 1976. These systems are typically constituted of two calendered, co-vulcanized layers of different rubber compounds. The top one is responsible for the aesthetics, the frictional behavior and wear/environmental resistance. The bottom one, whose characteristics govern the dynamic behavior of the track, affects instead the safety and performance of the athletes [2–8]. The production process of prefabricated tracks allows the introduction of honeycomb patterns or similar geometries to further enhance surface properties of a given material [9, 10].

Numerical modelling has been proposed [11–17] as a tool for optimizing the many variables defining the characteristics of sports surfaces: composition, relative thickness of the two layers and geometrical features. Such models are typically based on the approaches which have been successfully employed for this class of polymeric materials (rubber) in many different application fields [18–23].

So far, the most effective description of the dynamic behaviour of athletics tracks has been provided by a 3D finite element model, based on a visco-hyperelastic law to describe the constitutive behavior of the track material [24, 25]. An experimental protocol based on quasi-static compression testing was adopted to identify material parameters. Model predictions were validated against data from impact tests, performed on a conventional drop tower, as well as force reduction tests, conducted using an artificial athlete according to EN 14808:2005 [26]. A satisfying level of agreement between the experiments and numerical predictions was reported, with errors in the estimation of force reduction

✉ Luca Andena
luca.andena@polimi.it

1 Polymer Engineering Lab, Dipartimento di Chimica, Materiali e Ingegneria Chimica "Giulio Natta", Politecnico di Milano, Piazza L. Da Vinci, 32, 20133 Milan, Italy

2 Engineering, Exercise, Environment, Equipment for Sport (E4Sport) Lab, Politecnico di Milano, Piazza L. Da Vinci, 32, Milan, Italy

3 Mondo S.P.A., Piazzale Edmondo Stroppiana, 1, Alba, Italy

Published online: 07 August 2024

well within 10%. The model was then put to use to establish useful correlations between the dynamic response of the track and parameters of possible biomechanical interest [27]. Also, a preliminary exploration of the sensitivity of the surface dynamic characteristics to the dimensional features of the track geometrical pattern was conducted [10].

While viscoelasticity had been originally addressed in the first experimental studies on this matter [8, 14, 29], later studies demonstrated that the dynamic behavior of sports surfaces could be well described even by purely elastic models [11, 12, 15, 30]. This assumption is justified since any viscoelastic dissipation occurring within the material is captured during the experimental procedure which leads to the identification of the constitutive parameters, which are inherently altered to become fictitious, effective ones. Provided that the correct stretch rate is considered [10, 24], this approach works nicely during monotonic loading; however, once the load is removed, an even greater error occurs as the material further dissipates energy during the unloading phase. This error in the prediction of energy return characteristics limits the ability of the model to guide the optimization of the sports surfaces in terms of the final performance of the athlete.

To improve the overall accuracy, a model must explicitly include viscoelasticity. In the work of Andena et al. [31], an uncoupled model in which a Prony viscoelastic function modulates the time-response of the hyperelastic part was proposed. It provided a more accurate response during unloading [32], although a divergence between numerical predictions and experimental results was still reported.

Preliminary tests reported in [33] suggested that the origin of the error could be ascribed to the contribution of friction during compressive testing. Its influence could not be suppressed even when using proper lubrication between material samples and test plates. The present investigation deals with this effect of friction, which was investigated to identify a more robust experimental and modelling procedure and further increase the accuracy of the proposed framework. To this purpose, a series of experimental tests was conducted, aimed at measuring friction under various conditions and evaluating its effect on the compressive behavior of different rubber samples. The experimental activity has been supported by existing analytical models, detailed in the *Theoretical background* section.

2 Materials

Samples were supplied by MONDO SpA, Alba (CN, Italy) as 3 mm thick sheets. They were obtained by molding and vulcanizing in the company's laboratory three rubber compounds, based on different blends of natural rubber (NR), styrene-butadiene rubber (SBR) and ethylene-propylene-diene monomer rubber (EPDM). Their composition, while not exactly coincident with the formulation used for any existing commercial product, is within the range used for actual track materials: 6–15 wt% for NR and EPDM, and 20–30 wt% for SBR. The remaining weight fraction includes organic (wood flour, cellulose fibers) or inorganic (mainly talcum, calcium carbonate, silica, carbon black, kaolin, aluminum trioxide, magnesium dioxide) fillers, or a combination of both. Real tracks typically display an embossing on the top layer (to guarantee traction and water drainage) and a honeycomb pattern (hexagonal or square) at the bottom, to improve cushioning. Conversely, our lab sheets were plain, with a smooth surface and uniform thickness. The processing conditions selected for their preparation (with a vulcanization temperature of 170 °C held for 10 min.) mimic those experienced by the same compounds during production of the tracks. Some differences still remain, especially in terms of the final density obtained. The material in the tracks undergoes a certain level of expansion which determines an important degree of porosity in the final product (25–30%, according to the analysis reported in reference [31]).

Table 1 Materials investigated during the present study

Top layers		Bottom Layer	
Material	Density (kg/m^3)	Material	Density (kg/m^3)
F3	1386 ± 11	B3	1274 ± 19
F4	1304 ± 14		

Mean and standard deviation values out of 27 samples are reported

The need to keep the sheet processing conditions as close as possible to those of real tracks prevented the production of samples having higher thicknesses, with a more convenient aspect ratio for compressive testing. Moreover, such unfavorable aspect ratio is inevitable when dealing with samples obtained from actual tracks. While the track thickness is typically limited (usually between 10 and 15 mm), in-plane dimensions should be large enough to include a sufficient number of cells (given by the honeycomb pattern) to represent the sport surface as a whole.

Three different materials were investigated during this study, whose formulation is close to the typical ones used in either top (F3 and F4) or bottom (B3) layers.[1]

Table 1 reports the material list, together with density measured by weighting 27 samples of known volume for each material on an AS 310.R2 Radwag balance, with a 0.1 mg resolution.

[1] The nomenclature was chosen to avoid any confusion with the materials F1, F2, B1 and B2, reported in reference 33. These materials differ from the previously investigated ones.

Table 2 Summary of lubrication conditions applied during the experimental tests

Code	Lubricating medium
Steel	None (dry steel surface, cleaned before testing)
PTFE	Polytetrafluorethylene (PTFE) film with 0.2 mm thickness
PTFE + soap	Soap + water mixture on PTFE film with 0.2 mm thickness
Water*	Water on steel surface
Soap*	Soap + water on steel surface

*—tests on lubricated steel surfaces were conducted only at 10 mm/min

3 Experimental methods

Compressive and friction tests were performed on the selected materials. For both methodologies different lubrication conditions were applied, according to Table 2. The rubber compounds under study are unaffected by the liquid media considered (water and soap), which are typically employed for maintenance of these materials in the field.

Environmental conditions were controlled at 23 °C and 50% RH.

3.1 Friction tests

The coefficient of friction between a steel plate and the different rubber samples was measured using a method inspired by ASTM D1894 [34]; a sketch of the testing setup is shown in Fig. 1.

Square specimens measuring 50 × 50 × 3 mm were die-cut from the sheets and placed on the polished plate under a fixed weight of 12 N. The sliding plate was attached with a string via a pulley to the moving crosshead of an Instron 5967 Universal Testing Machine equipped with a 2 kN Instron 2580 loadcell with the K1 high-accuracy option, calibrated in class 0.5 down to 2 N. Three different speeds were used for each material: 1, 10 and 100 mm/min. This interval was chosen to be consistent with the range of sliding speeds experienced during compression testing (see below) under the hypothesis of material incompressibility. Two lubrication conditions (Water and Soap on steel) were included in this study at a later stage and tests were conducted at an intermediate speed of 10 mm/min.

Tests were run for a stroke of about 100 mm, except for those conducted at 1 mm/min, for which the displacement was limited to 40 mm to reduce testing times. For each condition (material/lubrication/speed), at least two replicates were performed.

The typical outcome of a friction test is shown in Fig. 2 for a specimen of material F4, at 100 mm/min and with no lubrication applied (dry steel surface). For each specimen, a steady-state region was visually identified following the initial transient. Within this range, the mean and standard deviation of the force reading were calculated to obtain the coefficient of friction, μ (μ = mean force/applied normal load). Preliminary testing allowed to estimate friction contributions arising from the pulley and wire system as negligible (less than 1%), compared to the typical force values observed during subsequent testing.

Some samples exhibited a stick–slip behavior during the first part of the test, especially at high speed and with no

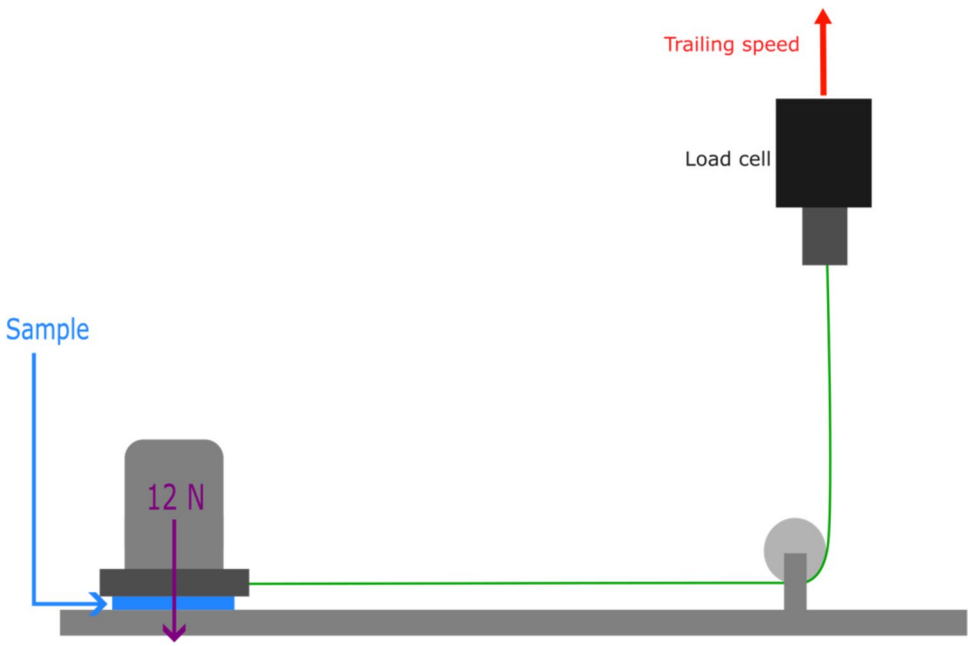

Fig. 1 Sketch of the friction testing setup

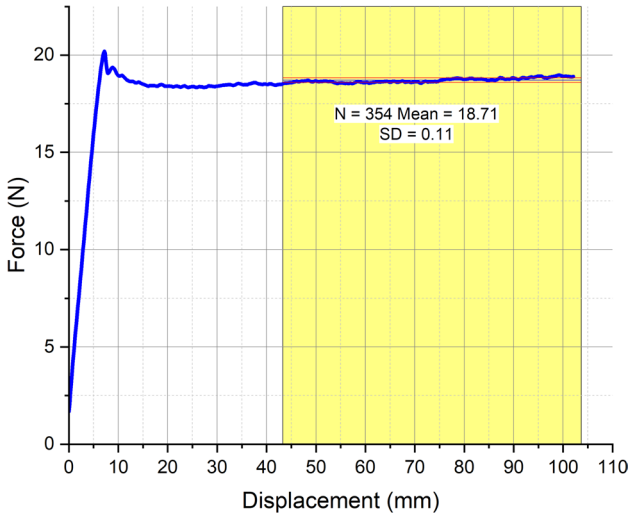

Fig. 2 Results of a friction test on a specimen of material F4 with no lubrication at 100 mm/min. The shaded area indicates the region where the mean force was calculated to evaluate the friction coefficient, equal to 1.55 in this case

applied lubrication. In these cases, the averaging was performed on the data acquired after the load was stabilized, ensuring that at least 300 data points were considered in the calculation. No attempt was made at identifying an accurate value for the static coefficient of friction, a task which would require more tests. Besides, steady-state conditions are more relevant to those experienced by specimens undergoing quasi-static compression tests at constant crosshead speed, as presented below.

3.2 Compression tests

Quasi-static compression tests were performed on an Instron 1185R5800 Universal Testing Machine equipped with a 100 kN Instron 2518 loadcell. Circular specimens having a diameter of 18 or 25 mm and thickness of 3 mm were die-cut from the sheets. The five lubrication conditions listed in Table 2 were applied between the steel compression plates and the top and bottom surfaces of the specimens. The only missing combination is the one with no lubricant (dry steel) on the 18 mm specimens. In the case of water and soap/water solution, samples were immersed during the test to ensure good contact between the liquid and their surface.

Three different crosshead speeds were selected to produce nominal deformation rates of 0.006, 0.06 and 0.6 s^{-1} on the 25 mm diameter specimens; for the 18 mm ones, only the intermediate speed was applied. The nominal deformation of the specimens is expressed through the stretch ratio $\lambda = {}^{L}/_{L_0}$, with L and L_0 being current and initial specimen height, respectively. It was calculated from the crosshead displacement after applying a correction for the compliance of the testing machine setup, which had been previously calibrated. The calibration procedure involved placing the compression platens directly in contact with increasing normal load, and recording the associated crosshead displacement. All tests were run down to $\lambda = 0.6$, with corresponding maximum loads ranging between 2 and 30 kN. A preload of 35 N was applied before each test to establish consistent contact conditions for all the specimens; this preload is negligible compared to actual loads recorded during the tests which were in the kN range. Three replicates were tested for each condition (material/diameter/lubrication/speed).

4 Theoretical background

The stress state in a rubber block during a compression test may differ substantially from ideal, uniaxial conditions because of a combination of high friction and compliance [35]. Friction at the interface prevents the block from properly expanding outwards. Under equilibrium conditions, a pressure gradient is generated, working against the expansion of the block, which adds to the stresses arising from and ideal (i.e., frictionless) compression. As a consequence, the apparent modulus measured in frictional compression exceeds the actual, "true" material's one; the difference becomes large for high friction coefficients and unfavorable aspect ratios (wide, thin blocks).

The problem of this artificial stiffening was addressed in reference [36], in which Gent and coworkers adapted a previous solution developed for bonded blocks [37]. Its derivation is based on the assumption of a linear elastic, incompressible material behaviour. The solution is valid for aspect ratios a/h higher than 1, with a being the block radius and h its thickness (see Fig. 3). With the inclusion of friction, outward slipping must be considered, depending on the actual value of the coefficient of friction, μ. The model does not make any distinction between static and dynamic friction conditions, which could be selected depending on the specific application. More details can be found in the Online Resource.

The main result of the analysis is the compressive force, F, needed for the deformation of the sample:

$$\frac{F}{\pi a^2 E e} = \left[\frac{R_1^4 a^2}{2h^2} + \frac{R_1^3 a}{\mu h} + \frac{R_1^2}{\mu^2} + \frac{R_1 h}{2a\mu^3} - \frac{h}{a\mu} - \frac{h^2}{2a^2\mu^2} \right] \quad (1)$$

where R_1 represents the radial distance r_1 at which the onset of slippage occurs, normalized with respect to a. Its value depends only on the aspect ratio and friction coefficient, and it can be determined from the following implicit relation:

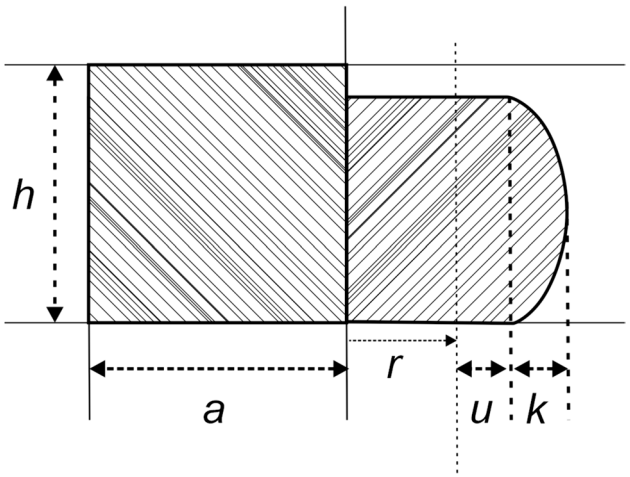

Fig. 3 Sketch of a section of a rubber block: in the left side, the rubber is undeformed, while in the right side is compressed; r represents the radial distance, u the slippage region and k the outward displacement

$$\frac{r_1}{\mu h} = e^{\frac{2\mu(a-r_1)}{h}} \tag{2}$$

The term $\pi a^2 Ee$ in Eq. 1 represents the contribution to the total force arising from the homogeneous compression. Hence, the right-hand side of Eq. 1 is the ratio of the apparent modulus (as measured during the compression test), E_a, to the true modulus of the material, E. The solution is valid for a/h ratio greater than unity, a condition which is satisfied for all the specimens tested during the present work.

5 Results

Test results are presented in a similar manner for both types (friction and compression): a comparison of the results obtained on the different materials/lubrication conditions is given first, followed by an analysis focused on the effect of speed/rate.

5.1 Friction tests

The raw force/displacement curves are reported in Fig. 4 for all materials and conditions; a comparison of the coefficient of friction values calculated for all the data at the common sliding speed of 10 mm/min is shown in Fig. 5. The different lubrication conditions considered display a trend common to all three materials, with friction forces decreasing in the following order: Steel → PTFE → Water → PTFE + soap → Soap. In particular, the forces measured on the dry steel surface are much higher than the rest; moreover, a marked stick–slip behavior is reported, especially at high speeds. The introduction of a PTFE sheet to act as a solid lubricant is somewhat effective in reducing friction, with values of μ which more than halved. Adding a liquid lubricant (water with and without soap) further reduces the measured forces.

When the most effective lubricant tested (soap + water) was applied, the μ values observed on steel were lower than those on PTFE. In fact, roughness may play an important role in this case, since the polished steel surface is smoother than that of the skived PTFE film. A lower roughness may prove beneficial once the lubrication is applied (despite the inherently stickier nature of the parent dry surface).

Finally, the effect of sliding speed is highlighted in the graph of Fig. 6, for the three surfaces on which tests were performed also at 1 and 100 mm/min. The velocity seems to have only a minor effect, with a slightly increasing trend observed for most conditions as this parameter is increased. The only exception are the data obtained at 100 mm/min on dry steel for the two finishing layers.

5.2 Compression tests

A comparison of the results obtained on all available combinations of material, lubrication and specimen diameter is presented in Fig. 7 for the compression tests at the intermediate stretch rate of 0.06 s^{-1}. The same trend observed in friction tests is confirmed, with stress values decreasing when moving from dry steel surfaces to soap lubricated ones. As expected, the response of the larger 25 mm diameter specimens is somewhat stiffer, because of the higher contact surface corresponding to their aspect ratio. Even the use of solid lubricant (PTFE) during compression testing of this type of rubber samples (with unfavorable aspect ratio and high friction) is not enough to avoid a large overestimation of the material stiffness. Another observation is that the condition producing the lowest friction values (Soap) also gives the most consistent results over the whole range of specimen material and size.

The next series of graphs is focused on data from 25 mm diameter specimens and three very different lubrication conditions: dry steel, dry PTFE and PTFE + water/soap solution. The data reported in Fig. 8 highlights the marked influence of testing rate on the mechanical response of the rubber samples. The effect of velocity may in principle arise from two independent phenomena: the inherent viscoelasticity of the materials and the rate dependence of friction. Yet, the former appears to be predominant, with an increase of the apparent stiffness which would not be justified according to the moderate sensitivity to speed reported in Fig. 6.

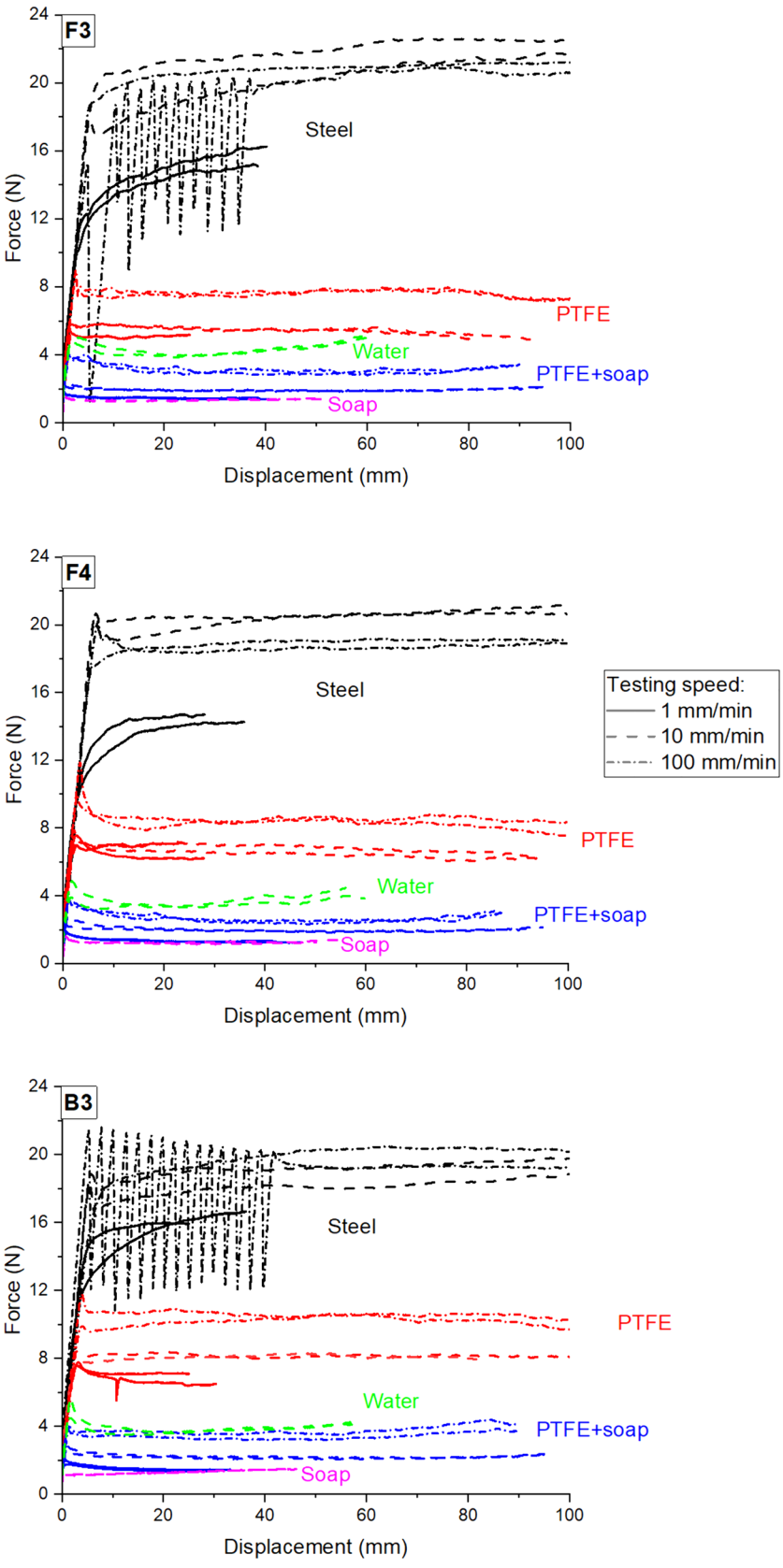

Fig. 4 Force vs. displacement data from friction tests for the different combinations of material, sliding speed and lubrication condition

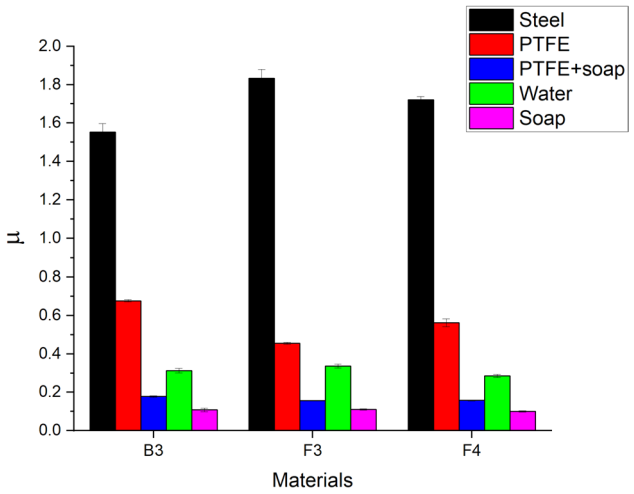

Fig. 5 Calculated coefficient of friction, μ, for the various combinations of material and lubrication. Mean values from the tests at 10 mm/min are reported, with the error bars representing the related standard deviation

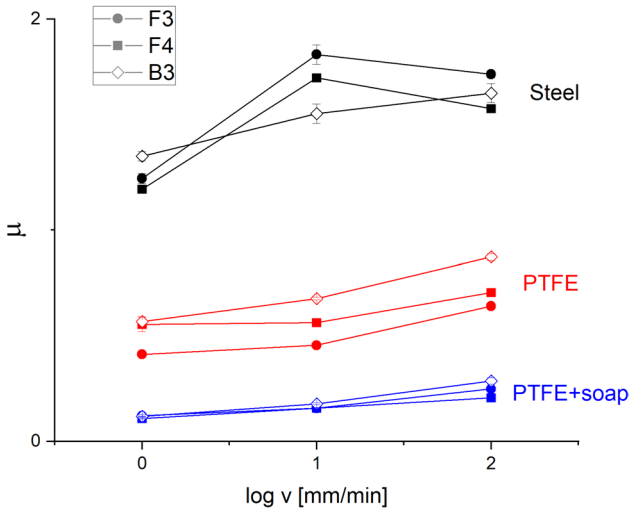

Fig. 6 Coefficient of friction, μ, as a function of the sliding speed for the three materials under study and three different lubrication conditions. Data points and error bars represent mean and standard deviation of relevant data

6 Discussion

While a region with a mostly steady-state regime could still be identified even on dry steel, the validity of these results would require additional confirmation. In particular, proper contact conditions (across the whole sample surface) must be verified and the presence of oscillations in the system should be excluded. The rubbery high-friction surface of relatively large, thin specimens affects the stress state during the tests. An artificial stiffening of the mechanical response is observed, which would provide a large overestimation of the stress-stretch response of the constituent materials. Use of a dry solid lubricant (PTFE film) is insufficient but also in presence of a water/soap mixture the friction coefficient is not negligible, with estimated values around 0.1–0.2. Such a level of friction is observed irrespective of the nature of the substrate employed, whether it is dry steel or again a PTFE film placed on it. Actually, data suggest that once good lubrication is applied, other factors may play a more important role (e.g., the surface roughness). Investigating the effect of the surface topography is however well outside the scope of the present study. The aim is not to correlate actual friction levels with surface properties, while to correctly account for it during mechanical characterization.

The aim of the experimental characterization in compression is to provide data which represent the intrinsic behaviour of constituent material. The issue of friction prevents direct access to this intrinsic constitutive behavior, and moreover the material parameters which could be identified from the data depend on specimen geometry via their aspect ratio. While in principle the stiffening effect of friction could be further reduced, its suppression to negligible levels would be hardly feasible and probably impractical, in terms of the additional complexity required during testing.

A possible solution is given by the application of the Gent model presented in the Theoretical background section. Building on the experimental direct measurements of the friction coefficients corresponding to each relevant condition of material/lubrication/speed, the model can be applied to compression data to extrapolate virtual "frictionless" curves, representing the true material behavior. Any identification procedure aimed at obtaining relevant material constitutive parameters will then be applied on the frictionless data, and used in conjunction with numerical models in which friction is explicitly reintroduced in a subsequent stage, according to the actual conditions which the simulations aim to reproduce.

To validate the applicability of the proposed approach, the following procedure was developed:

I. A single lubrication condition was selected as the reference one; in the present case, the choice fell on the one which exhibited the lowest friction values (water/soap mix on steel).
II. For such a reference condition, the stress ratio predicted from Eq. 1 was assumed to be valid, and the corresponding frictionless curve was obtained by applying this ratio to the mean experimental stress (from the three replicates), for each stretch value, λ.

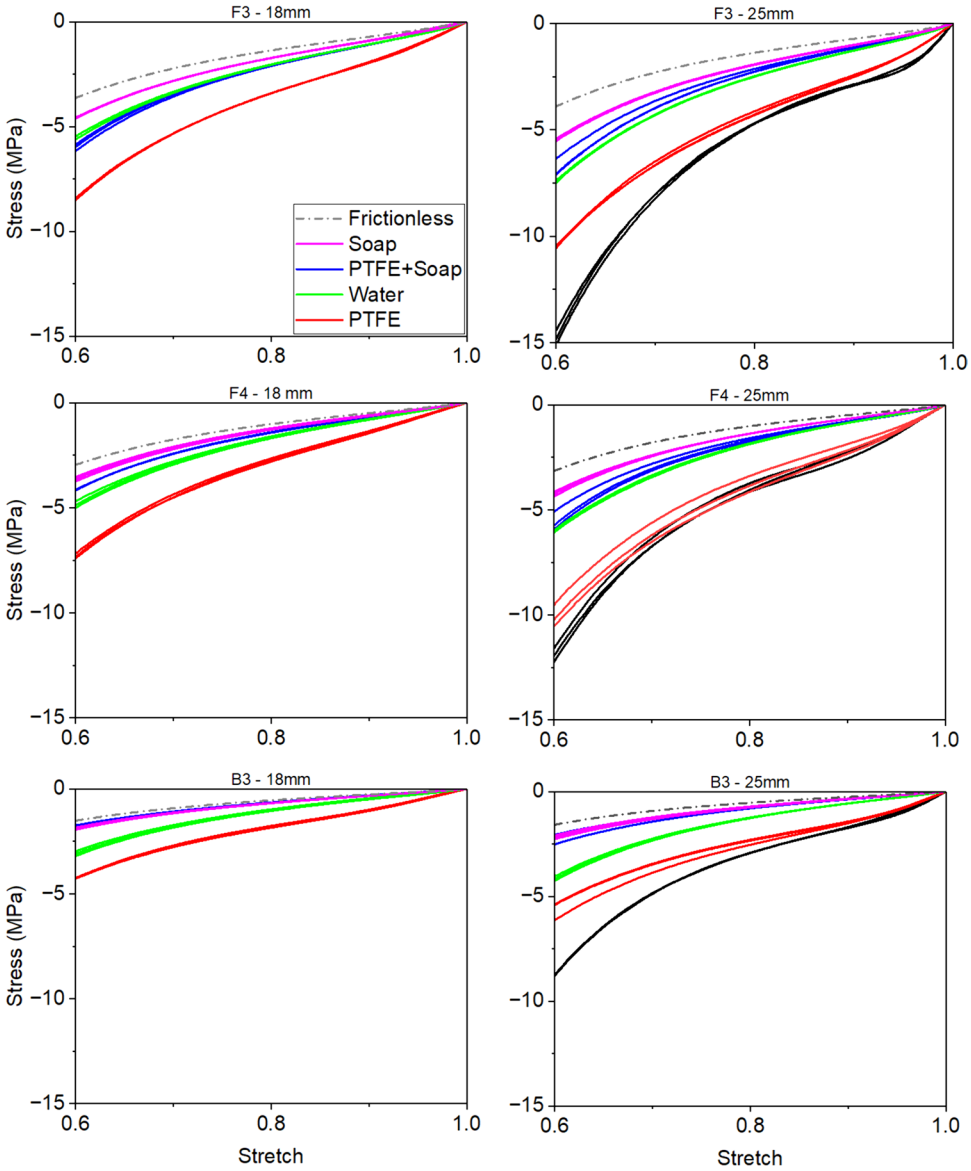

Fig. 7 Nominal stress vs. stretch data from compression tests at the intermediate stretch rate of 0.06 s^{-1}, for all materials and applied lubrication conditions and both sample diameters (18 and 25 mm). Stress values are negative and stretch is less than unity because of the compression state (curves originate from (1;0). Frictionless curves generated by applying the correction proposed by Gent [37] to data obtained using the Soap configuration, as according to the procedure detailed in Sect. 6

III. For the other lubrication conditions, the ratio of the mean stress over the frictionless stress was calculated at each λ.
IV. Mean and standard deviation values of these ratios over the whole range of λ were calculated and plotted as a function of the coefficient of friction, as measured via relevant friction tests performed in the same lubrication condition.

The method was applied to the three materials, considering both datasets (18 and 25 mm diameter) and the intermediate rate of 0.06 s^{-1}, for which the broadest set of conditions was investigated. The outcome of the analysis is plotted in Fig. 9, compared with the analytical prediction offered by the Gent model (Eq. 1). Obviously, for each diameter the data points corresponding to the reference condition (one for each of the three materials) collapse on the analytical curve.

For values of μ smaller than 0.4 (typical of lubricated conditions), there is a good agreement between the experimental data and the model. As μ increases, the latter appears to overestimate the actual stiffness measured during the tests. This trend is evident in the case of dry PTFE, where a higher data dispersion when averaging over the different λ values is also visible for the larger diameter. In the case of dry steel (for which data is available only on 25 mm samples), μ values lie between 1.5 and 2, and the model prediction is inaccurate. However, as mentioned in Sect. 5.1, reported experimental issues may have compromised the accuracy of the original data. Moreover, the roughness of the compression plates differs from that of the plate used during friction tests. A further element which may contribute to the reported

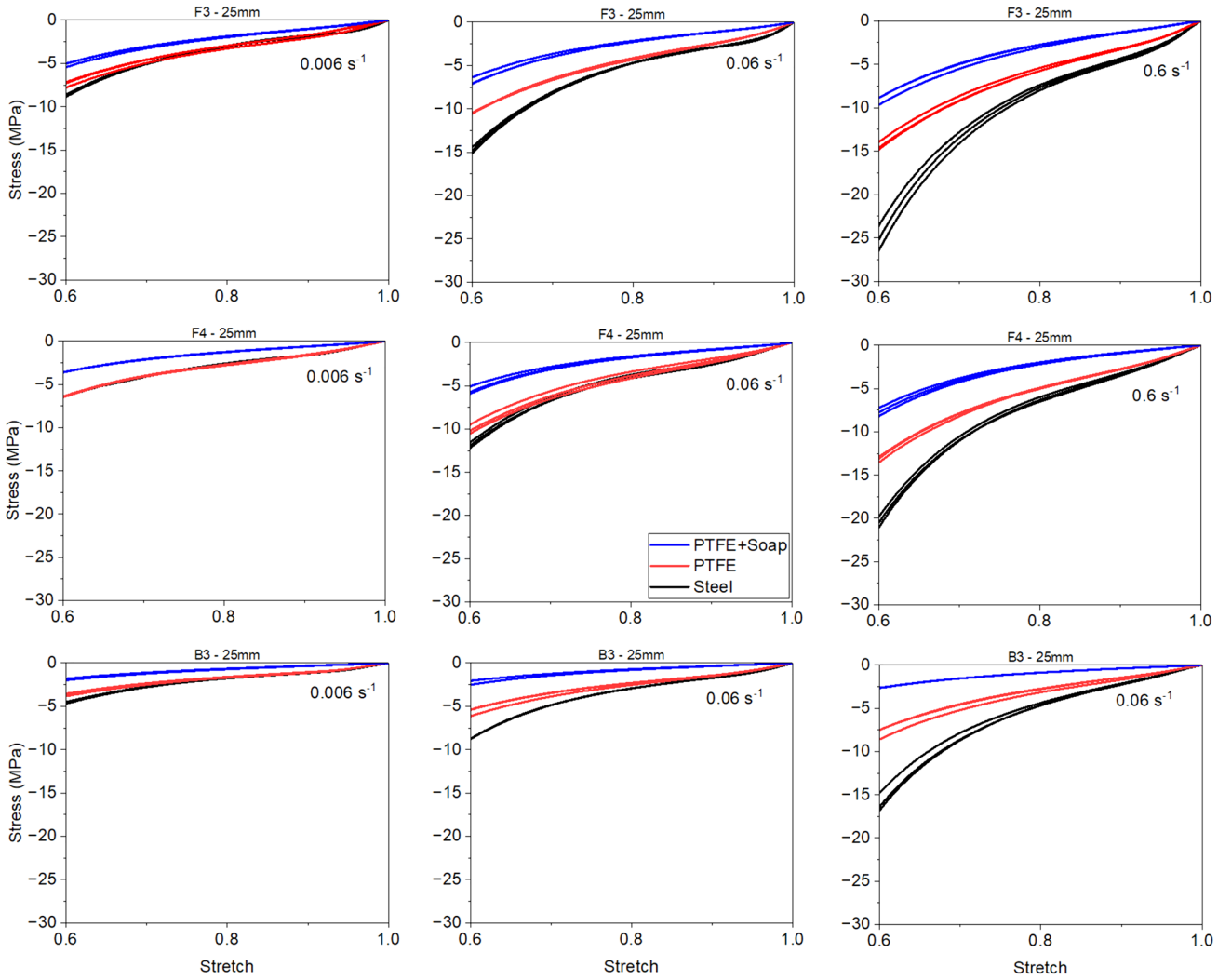

Fig. 8 Effect of speed on the compressive behavior on the three investigated materials for 25 mm diameter specimens and three selected lubrication conditions (dry steel, dry PTFE and PTFE + soap/water mix)

mismatch is the widely different levels of contact pressure between the two types of tests. The difference exceeds an order of magnitude, and the real contact area can be influenced, especially for higher friction coefficients. For these reasons, we excluded data on unlubricated surfaces from our analysis, which explains why tests on 18 mm diameter samples were not performed on dry steel. The frictionless over friction ratio was considered as a relevant parameter for lubricated surfaces. The mean error between analytical predictions and experimental measurements goes from about 10% to 20% for 18 mm and 25 mm diameter, respectively.

Still, the agreement between model and experiments for lower values of μ confirms the validity of the proposed procedure. Equation 1 can well describe the influence of friction on the apparent stiffness measured during a compression test, irrespective of the specific material tested and specimen dimensions. It is therefore possible to take the frictionless curves built during step II of the proposed procedure, and assume them as representative of the sought intrinsic material behaviour; they are presented as dashed lines in Fig. 7. They could then be employed even if the field conditions differ from those of the original compression tests, provided the correct geometry and friction values are considered in the analysis. For example, they could be used to predict the behavior of rubber surfaces even at rates for which the friction coefficient could deviate from the values measured in quasi-static tests. One would only require to measure friction in the relevant conditions, and then include this information in a model which—thanks to the frictionless curves—provides a more accurate estimate of the true compressive properties of the material. The use of these frictionless curves to model the mechanical behaviour of sports surfaces will be

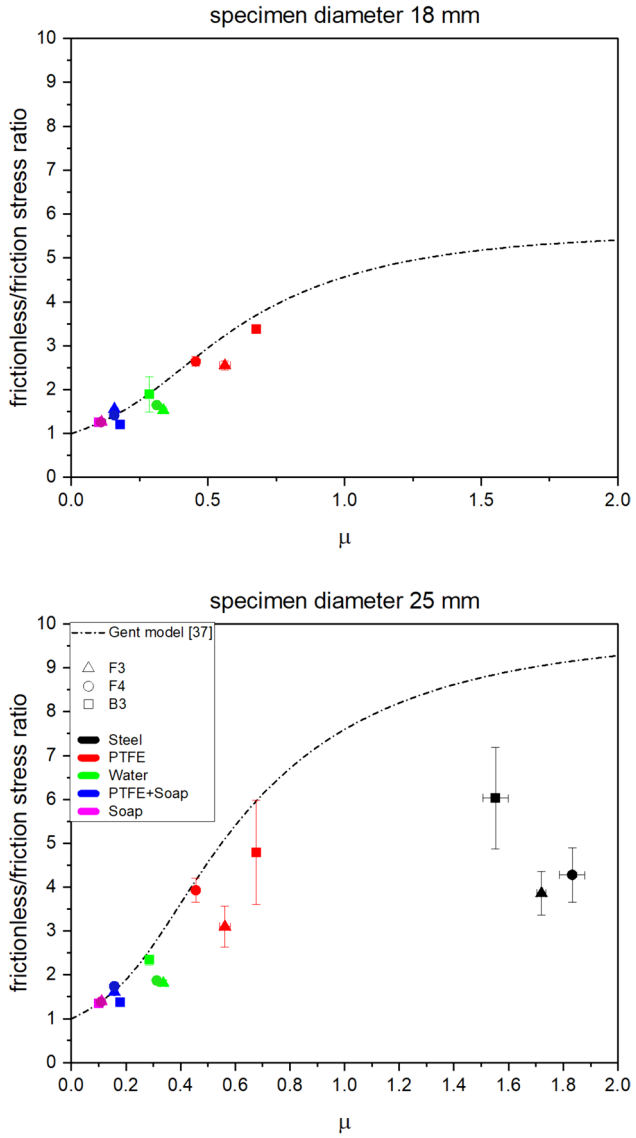

Fig. 9 Comparison of the analytical prediction of the Gent model [37] with the data obtained at the intermediate rate of 0.06 s^{-1}, for both specimen diameters, on all available materials and conditions. The ratio between the apparent stress and the "true", frictionless stress is plotted. The "Soap" lubrication condition (water + soap on steel) was chosen as the reference configuration. Error bars represent the uncertainly in the determination of the stress ratio (mean for all stretch values) and of the friction coefficient (from the related experiments)

the subject of another research paper, focused on the finite element modelling aspects.

The proposed approach worked for values of μ below unity: this limitation is not related to any limitation present in the Gent model. It is rather a consequence of the difficulty of correctly evaluating friction values with our setup, in a way which is consistent with the actual conditions applied during compression testing.

7 Conclusions

The present investigation addresses the problem of identifying the mechanical behaviour of rubbers from compression tests, performed on specimens having unfavorable geometry. The reported friction data displays large variations of the measured coefficient of friction, with values ranging from 0.1 to 1.8. These fluctuations in the level of friction experienced by flat compression specimens produce a dramatic effect on their apparent mechanical properties, and induce a strong dependence on specimen geometry. The proposed solution is to apply the analytical model proposed by Gent to describe the apparent stiffening effect induced by friction. The results obtained support the validity of the model within a relatively broad range of conditions (in terms of materials, friction levels and aspect ratio). The procedure allows the creation of virtual "frictionless" curves by rescaling experimental data for the stiffening factor predicted by Gent model. These curves represent the intrinsic behavior of the material, as could be determined by an ideal experiment in which friction was completely suppressed. They can be used as a reliable input to describe the rubber behaviour in numerical models developed for various applications.

Supplementary Information The online version contains supplementary material available at https://doi.org/10.1007/s12283-024-00471-7.

Acknowledgements The authors wish to thank Oscar Bressan and Dr. Marco Contino for their contribution to the experimental part of this work; Filippo Cotta Ramusino and Profs. Andrea Pavan, Francesco Briatico, Stefano Mariani for their scientific advice.

Funding Open access funding provided by Politecnico di Milano within the CRUI-CARE Agreement. Luca Andena reports financial support was provided by Mondo S.p.A.

Data availability Data will be made available on reasonable request, subject to approval by Mondo S.p.A. for what pertains to proprietary information.

References

1. World Athletics, Track and Field Facilities Manufacturing, 2019 edition, 2019.

2. McMahon TA, Greene PR (1979) The influence of track compliance on running. J of Biomech 12:893–904
3. Nigg BM, Yeadon MR (1987) Biomechanical aspects of playing surfaces. J of sports sci 5:117–145
4. Baroud G, Nigg BM, Stefanyshyn D (1999) Energy storage and return in sport surfaces. Sports Eng 2:173–180
5. Stefanyshyn DJ, Nigg BM, Cole GK (2003) Sport surfaces: biomechanics, injuries, performance, testing, installation. University of Calgary, Human Performance Laboratory. ISBN: 0889532680, 9780889532687
6. Daoud AI, Geissler GJ, Wang F, Saretsky J, Daoud YA, Lieberman DE (2012) Foot strike and injury rates in endurance runners. Off J Am Coll Sports Med 44:1325–1334
7. Zadpoor AA, Nikooyan AA (2011) The relationship between lower-extremity stress fractures and the ground reaction force: a systematic review. Clin Biomech 26:23–28
8. Benanti M, Andena L, Briatico-Vangosa F, Pavan A (2013) Viscoelastic Behavior of athletics track surfaces in relation to their force reduction. Polym Test 32:52–59
9. Wang H, Zheng W, Ma Y, Tang Y (2019) Shock absorption properties of synthetic sports surfaces: a review. Polym Adv Technol 30:2954–2967
10. Andena L, Aleo S, Caimmi F, Mariani S, Briatico-Vangosa F, Pavan A (2016) A 3D numerical model for the optimization of running tracks performance. Procedia Eng 147:854–859
11. Kim S, Shin HO, Yoo DY (2020) Mechanical and dynamic behavior of an elastic rubber layer with recycled styrene-butadiene rubber granules. Polym 12:3022–3037
12. Thomson RD, Birkbeck AE, Lucas TD (2001) Hyperelastic modelling of nonlinear running surfaces. Sports Eng 4:215–224
13. M. J. Carré, D. M. James, S. J. Haake (2006), Hybrid Method for Assessing the Performance of Sports Surfaces During Ball Impacts Proceedings of the Institution of Mechanical Engineers. Part L J Mater Des Appl 220: 31–39.
14. Kobayashi K, Yukawa H (2011) Identification of the exponential function type nonlinear voigt model for sports surfaces by using a multi-intensity impact test. J of Syst Des and Dyn 5:1326–1336
15. Cole D, Forrester S, Fleming P (2018) Mechanical characterisation and modelling of elastomeric shockpads. Appl Sci 8:501–513
16. Forrester S, Fleming P (2019) Traction forces generated during studded boot-surface interactions on third-generation artificial turf: a novel mechanistic perspective. Eng Rep 1:e12066
17. Cole D, Fleming P, Morrison K, Forrester S (2020) Evaluation of the advanced artificial athlete and Hall effect sensors for measuring strain in multi-layer sports surfaces. SN Appl Sci 2:484–497
18. Tomin M, Kossa A, Berezvai S, Kmetty A (2022) Investigating the impact behavior of wrestling mats via finite element simulation and falling weight impact tests. Polym Test 108:107521
19. Busfield JJC, Deeprasertkul C, Thomas AG (2000) The effect of liquids on the dynamic properties of carbon black filled natural rubber as a function of pre-strain. Polym 41:9219–9225
20. Plagge J, Klüppel M (2017) Mullins effect revisited: relaxation, recovery and high-strain damage. Int J of Plasticity 89:173–196
21. Carleo F, Barbieri E, Whear R, Busfield JJC (2018) Limitations of viscoelastic constitutive models for carbon-black reinforced rubber in medium dynamic strains and medium strain rates. Polymers 10:988. https://doi.org/10.3390/polym10090988
22. De Tommasi D, Puglisi G, Toma E, Trentadue F (2019) A predictive model for the hysteretic and damage behavior of rubberlike materials. J of Rheol 63:1–10
23. Bazkiaei AK, Shirazi KH, Shishesaz M (2020) A frame-work for model base hyper-elastic material simulation. J of Rubber Res 23:287–299
24. Andena L, Briatico-Vangosa F, Ciancio A, Pavan A (2014) A finite element model for the prediction of force reduction of athletics tracks. Procedia Eng 72:847–852
25. Andena L, Briatico-Vangosa F, Cazzoni E, Ciancio A, Mariani S, Pavan A (2015) Modeling of shock absorption in athletics track surfaces. Sports Eng 18:1–10
26. EN 14808:2005, Surfaces for sports areas. Determination of shock absorption, 2005
27. L. Andena, A. Ciancio, F. Briatico-Vangosa, S. Mariani, A. Pavan (2018), On the relationship between force reduction, loading rate and energy absorption in athletics tracks. Proc Inst Mech Eng Part P J Sports Eng Technol 232: 71–78
28. Andena L, Aleo S, Briatico-Vangosa F, Mariani S, Tagliabue S, Pavan A (2018) Modelling the cushioning properties of athletic tracks. Sports Eng 21:453–463
29. Durá JV, García AC, Solaz J (2002) Testing shock absorbing materials: the application of viscoelastic linear model. Sports Eng 5:9–14
30. M Mehravar, P Fleming, D Cole, S Forrester (2016) Mechanical characterisation and strain rate sensitivity of rubber shockpad in 3G artificial turf, Proc. of the 24th UK Conf of the Assoc for Comput Mech in Eng Cardiff University
31. L Andena, F Cotta Ramusino, S Tagliabue, S Zalaffi (2022) A visco-hyperelastic numerical model for the dynamic behaviour of rubbers, Const Model for Rubber XII, Milano, Italy, 71–277
32. Goh SM, Charalambides M, Williams JG (2004) Determination of the constitutive constants of non-linear visco-elastic materials. Mech Time-Depend Mater 8:255–268
33. S Zalaffi (2021) Accounting for friction in the characterization of synthetic sports surfaces. MSc Thesis, Politecnico di Milano
34. ASTM D1894, Standard test method for static and kinetic coefficients of friction of plastic film and sheeting, 2014
35. Gere JM, Timoshenko SP (1997) Mechanics of materials, 4th edn. PWS Publishing Company, Boston
36. AN Gent, FM Discenzo, JB Suh (2009) Compression of rubber disks between frictional surfaces, Rubber Chem and Technol Const Model for Rubber VI, London, UK, 821–17.
37. Gent AN, Lindley PB (1959) The compression of bonded rubber blocks. Proc Inst Mech Eng 173:111–122